August 2003 • NREL/SR-500-33249

Subcontractor Report

Minimization of Motion Smear: Reducing Avian Collisions with Wind Turbines

Period of Performance: July 12, 1999 – August 31, 2002

W. Hodos
University of Maryland
College Park, Maryland

National Renewable Energy Laboratory

1617 Cole Boulevard
Golden, Colorado 80401-3393

NREL is a U.S. Department of Energy Laboratory
Operated by Midwest Research Institute • Battelle • Bechtel

Contract No. DE-AC36-99-GO10337

August 2003 • NREL/SR-500-33249

Minimization of Motion Smear: Reducing Avian Collisions with Wind Turbines

Period of Performance: July 12, 1999 – August 31, 2002

W. Hodos
University of Maryland
College Park, Maryland

NREL Technical Monitor: K. Sinclair

Prepared under Subcontract No. XAM 9-29211-01

National Renewable Energy Laboratory

1617 Cole Boulevard
Golden, Colorado 80401-3393

NREL is a U.S. Department of Energy Laboratory
Operated by Midwest Research Institute • Battelle • Bechtel

Contract No. DE-AC36-99-GO10337

Acknowledgments

The principal investigator would like to thank Karin Sinclair of NREL for her encouragement, support, and guidance during the course of the project. Michael Morrison's experience, insights, and suggestions were of great value in planning various aspects of the research and in interpreting the data.

Alex Potocki, Thilo Storm, Matthew Zimmerman, and Matthew Gaffney provided excellent technical assistance and expertise in the collection, analysis, and interpretation of the data. Mimi Ghim provided useful technical suggestions at several critical points in the research.

This research could not have been carried out without the cooperation of John French of the Patuxant Wildlife Research Center in Beltsville, MD, who generously allowed us to borrow and study American kestrels from his facility and advised us on their care and handling.

Dr. Katherine Nepote, Director of Laboratory Animal Care at the University of Maryland, College Park, provided veterinary support during the planning and execution of the research.

Executive Summary

Collisions with wind turbines can be a problem for many species of birds. Of particular concern are collisions by eagles and other protected species. This research study used the laboratory methods of physiological optics, animal psychophysics, and retinal electrophysiology to analyze the causes of collisions and to evaluate visual deterrents based on the results of this analysis. Bird collisions with the seemingly slow-moving turbines seem paradoxical given the superb vision that most birds, especially raptors, possess. However, our optical analysis indicated that as the eye approaches the rotating blades, the retinal image of the blade (which is the information that is transmitted to the animal's brain) increases in velocity until it is moving so fast that the retina cannot keep up with it. At this point, the retinal image becomes a transparent blur that the bird probably interprets as a safe area to fly through, with disastrous consequences. This phenomenon is called "motion smear" or "motion blur" and is well known in human visual perception.

Based on this analysis, we devised a variety of patterns intended to give the retina more time to "rest" between successive stimulations by the blades. These patterns include various staggered-stripe patterns on a three-blade array, as well as a single black blade paired with two white blades. Several of these patterns increased the visibility of the blades. Nevertheless, above a critical retinal-image velocity, even these patterns lost their visibility advantage and became blurred. Using our data, we were able to model the distances at which patterns maintain their visibility for different turbine diameters and rotation rates. Although it seems counterintuitive, the stimuli lose their visibility at greater distances from the larger-diameter, slower-rotating turbines than from the smaller, faster types. Thus, an anti-motion-smear pattern that maintained its visibility as close as 20 m for a small, fast turbine would lose visibility closer than 50 m for a large, slow turbine.

Another series of experiments involved the use of single-colored blades instead of single black blades. In addition, various chromatic and achromatic single blade types were evaluated against naturalistic backgrounds composed of color photographs of wind turbines in various types of sky and foliage configurations. Although these studies indicated that color contrast was a critical variable (i.e., that the effectiveness of a colored blade depended on the color of the background against which it was viewed), the applicability of their results to the real world of birds is limited. First, the background was always stationary, whereas in nature, the background seen by a flying bird is always moving. Second, the colors in photographs may be accurate for the human eye, but avian color vision is quite different from human color vision, and color photographs may not accurately represent the colors seen by birds and may not have appeared natural to them. Given these uncertainties, in those conditions in which the background color changes rapidly depending on the moment-to-moment view point of the bird, black would probably be the best compromise color, even though it was not as highly visible compared to colors such as blue and green against a fixed background in a laboratory simulation.

Finally, we tested a series of devices applied to the blade tips to deter collisions from a lateral approach to the blades. Attaching tips to two of the three blades clearly improved visibility against the neutral background, but less so against a naturalistic background. Although the results of the naturalistic background studies were inconclusive, they did suggest that such devices might be effective under certain circumstances.

It is important to note that these studies have only evaluated the visibility of anti-motion-smear blade patterns and not their ability to deter a flying raptor from approaching them. Deterrence is a psychological property of a pattern that can only be evaluated in an awake, behaving bird, not in an anesthetized bird, as was the case in our studies. The deterrent effect of these patterns can best be tested in a field setting by observing the behavior of the birds and by determining the before and after fatality rates at turbines that have been treated with various patterns versus untreated, fatality-matched turbines.

In our opinion, the results of the laboratory visibility simulations were sufficiently encouraging. We recommend a field test of a single-blade, solid black pattern or a single-blade, thin-stripe pattern as the next step to determine whether the patterns are effective in reducing fatalities.

Table of Contents

Table of Figures

Table of Tables

Introduction

The development of wind power for the generation of electricity led to the establishment of "wind farms," such as the Altamont Wind Resource Area in California, in which thousands of wind turbines have been erected. While generally conceded to be environmentally safe, wind turbines have been reported to be hazardous to flying birds (Howell, 1991; Colson & Associates, 1995; NREL wind power meeting proceedings**,** 1994 and 1995; Thelander and Rugge, 2000). The purpose of the research described here was to develop a method for rapidly screening various blade patterns to deter bird collisions. The research was designed to take into account what is known from human research on the degradation of the perception of rapidly moving objects.

Visual Hypotheses to Account for Collisions

Failure to Divide Attention

One possible explanation for avian collisions is the birds' inability to divide their attention between surveying the ground for prey and monitoring the horizon and above for obstacles; i.e., they are so busy searching the ground that they do not notice the turbines. This hypothesis derives from substituting our knowledge of human vision for that of avian vision. Humans are foveate animals; we search the visual world with a small area of the retina known as the fovea, which is our area of sharpest vision, like someone searching a dark room with a narrow-beam searchlight. This results from our very low ratio (approximately 1:1) of photoreceptors to ganglion cells in the macular region of the retina. Outside the macular region, the ratio of receptors to ganglion cells increases progressively to 50:1 - 100:1, and our visual acuity drops sharply. Birds and many other animals, on the other hand, have universal macularity, which means that they have a low ratio of receptors to ganglion cells (4:1 - 8:1) out to the periphery of the retina. They maintain good acuity even in peripheral vision (Hodos, Miller, and Fite, 1991; Hodos, 1993). In addition, raptors possess the specialization of two foveal regions: one for frontal vision and one for looking at the ground. Moreover, birds have various optical methods for keeping objects at different distances simultaneously in focus on the retina (Hodos and Erichsen, 1990). Because of these considerations, failure to divide attention seems like an unlikely hypothesis.

Motion Smear: Reduced Visibility of the Blades, Especially at the Tips

As an object moves across the retina with increasing speed, it becomes progressively blurred; this phenomenon is known as "motion smear," "motion blur," or "motion transparency" and is well known in human psychophysical research. It results because the human visual system is sluggish in its response to temporal stimulation; i.e., the visual system (in humans) summates signals over periods of about 120 msec in daylight (Burr, 1980; Bex et al., 1995).

The phenomenon of motion smear is apparent at the tips of wind turbine rotor blades as the observer (bird, human, or camera) approaches the turbine. Motion smear is not apparent in the central regions of the rotors. Even though the central regions and the tips are rotating at the same number of revolutions per minute (RPM), the absolute velocity of the blades is much higher at the peripheral regions. The higher velocity of the blade tip has placed it in the temporal-summation zone, in which the retina is sluggish in its ability to resolve temporally separated stimuli, whereas the lower velocities of the more central portions are below the transition point between blur and non-blur; the individual blades thus can be seen more or less clearly. Moreover, the absolute velocity of the blade in the visual world is not critical; rather, it is the absolute velocity of the image of the blade that sweeps across the retina that is the critical variable. For reasons that will be explained later in this introduction, as the observer approaches the turbine, the retinal image of the blades increases in velocity until the retina can no longer process the information. This results in motion smear or motion transparency—the blade becomes transparent to the viewer. This transparency is illustrated in Fig. 1, which was photographed at the Altamont Wind Resource Area. Observe the blade on the left of the turbine in the center foreground of the photo. One can clearly see a distant turbine behind the outer one-third of the blade of the foreground turbine as if the blade were virtually transparent. A solution to avian collisions with wind turbines must take into account the causes of motion smear and consider whether blade patterns could minimize this effect.

Figure 1. An illustration of the effect of distance on motion smear. The blade on the left of the turbine in the foreground is nearly transparent because of motion smear resulting from a slow shutter speed on the camera. The turbine directly behind this blade is clearly visible. At an even closer distance to the foreground turbine, its blades would become virtually invisible.

The Theory of Motion Smear

One of the characteristics of motion smear is that it eliminates the high spatial frequencies from visual patterns, which is why they appear to go out of focus and become virtually transparent (Steinman and Levinson, 1990). High spatial frequencies are those Fourier components of a visual object that are found at edges and corners and in fine details. The print on this page, for example, is made up mainly of high spatial frequencies. If they are removed by optical blur or refractive error, the text becomes transparent and, in the worst case, virtually disappears.

The Law of the Visual Angle

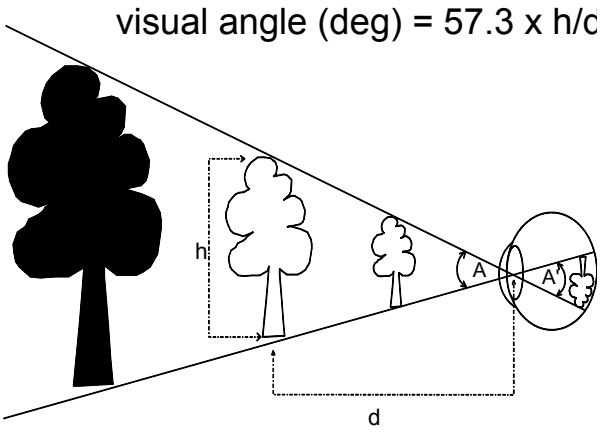

Figure 2. The law of the visual angle. Objects of different sizes and distances that subtend the same angle will cast the same size image on the retina. Angles A and A' are the same.

Fig. 2 shows how objects of different sizes and different distances can form the same size image within the eye. The angle (A') inside the eye is the same as the angle (A) from the eye to each of the objects. These angles, called "visual angles," are the conventional units to describe object size because they are directly related to retinal-image size, which is the only relevant variable for these purposes. Thus, a small object close to the eye can cast the same size retinal image as a large object seen from a much farther distance.

In the experiments described later, the tip velocity will be the velocity of the retinal image of the blade (which is the information that is actually transmitted from the eye to the brain) and will be expressed in degrees of visual angle/sec (dva/sec). Degrees of visual angle are calculated as 57.3 x h/d, in which h is the object size (height, width, or area), d is the distance, and 57.3 is the conversion factor from radians to degrees. The advantage of measurements in degrees of visual angle for laboratory research is that the tip velocity of a rotor blade many meters in length as seen from a distance of 10-20 m can be simulated in the laboratory with a much smaller blade located 0.5-0.6 m from the eye and moving at a much higher RPM rate.

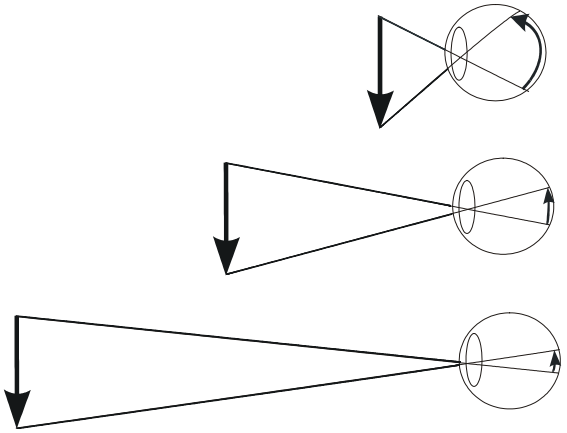

Figure 3. As an observer, such as a bird, gets closer to an object, the object's retinal image increases in size. If the object is moving, the retinal image when close must cover a greater distance on the retina in the same amount of time, resulting in a greater retinal image velocity.

As seen in Fig. 3, an object of an unchanging size will cast a retinal image whose size is dependent on the distance. As the bird approaches the rotor blades, the size of the blades' retinal image increases, just as a photographic image increases in size as the camera approaches the subject. This means that as the bird approaches the rotor blades, its retinal velocity increases because the tip of the blade must cover a greater distance in the same time. This is related to the phenomenon of "motion parallax" (Goldstein, 1984), which we can observe by looking out the side window of a rapidly moving train or car. Objects close to the window race by with great speed and have a considerable motion smear, while distant objects move at a more leisurely pace and remain sharply in focus. An ideal visual deterrent for avian-turbine collisions is one that continues to provide high visibility as the

bird gets closer to the whirling blades. Our analysis of the problem from the velocity-detection literature and from our own experiments reported here indicates that the physiology of the retina will not permit such a situation. Beyond a certain point, the velocity of the retinal images of the blades sweeping across the retina will overwhelm the retina's ability to keep up. The initial effect will be a smearing or blurring of the image of the blades. They may finally appear transparent and look like a safe place to fly, with deadly consequences for the bird.

The Principle of Motion Smear Reduction

A partial solution to the problem of motion smear is to maximize the time between successive stimulations of the same retinal region. Patterns applied to the blades that do not take this into account may have reduced effectiveness in deterring avian collisions. The typical approach is to apply the same pattern to each blade, which does little to maximize the time between successive stimulations of the same retinal region. Our approach has been to use different patterns on each blade. The patterns are designed so that a pattern on any given blade region is not repeated on the equivalent region of the other two blades. Thus stimulations per second of any given retinal region are reduced by a factor of 3, and the time between stimulations should be approximately tripled.

Motion Smear Reduction to Frontal Approaches to the Blades

Fig. 4 shows an illustration of one such type of blade pattern. The figure shows seven concentric virtual rings into which a drawing of rotor blades has been placed. Each ring has only one blade bar, and no two blades have a bar in the same location. We have constructed such a rotor-blade assembly and mounted it on a variable-speed motor. As the speed of the motor increases, human observers report that the individual bars at the more peripheral regions of the blade are no longer seen as individual bars. They are gradually replaced by a series of grey, concentric rings that pulsate slightly. The spaces between the rings, however, continue to show the transparency associated with motion smear. The effect is quite dramatic at high tip velocities. Blades on which the bars have been placed at the same location on all blades, or blades that are uniformly white or uniformly black, show the typical motion-smear effect.

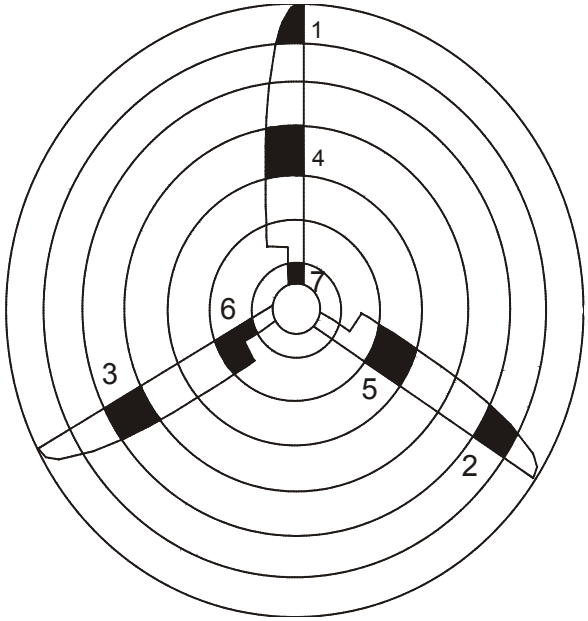

Figure 4. An anti-motion-smear pattern. A black bar on one blade is not repeated in the same location on the other two blades.

A second type of pattern that meets the criteria for an anti-motion-smear pattern is shown in Fig. 5. In this pattern, each of the staggered segments has been collected onto a single blade, which results in a solid black blade. This pattern offers a practical advantage: painting a turbine with this pattern would require the uniform painting of a single blade, instead of precision application of paint to three blades. This pattern and several other pattern types were tested for visibility in American kestrels using a method based on the physiology of the retina. The patterns and the results are presented in Experiments 1, 2, and 3.

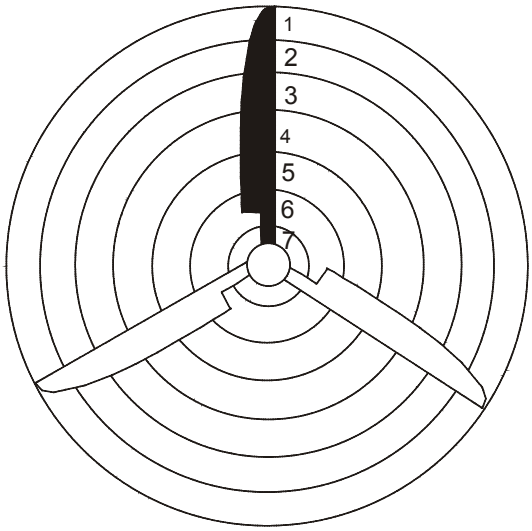

Figure 5. A single-blade, anti-motion-smear pattern.

Angle of Approach to the Blades

A serious problem in attempting to solve the problem of collisions is the absence of data on the bird's angle of approach to the blades at the moment of collision. If the birds are struck while approaching the blades from a direction that is parallel to the long axis of the blade, then the problem of motion smear is compounded by the very small profile of the blades from that line of sight. A solution to this problem must (1) effectively increase the profile of the blades in this orientation, and (2) take into account the causes of motion smear.

Motion Smear Reduction in Lateral Approaches to the Rotor Blades

The combination of motion smear and a very narrow profile offered by the fast-moving tips of rotor blades approached from the side could be deadly for a bird. One possible solution to this problem is a rectangular attachment to the outer tip of the blade. This attachment is fastened to be at right angles to the long axis of the blade (see Fig. 6). The attachment ideally would be positioned on only one blade to minimize motion smear. If a single device causes an imbalance of the rotor assembly, additional rectangles could be added to the other two blades for balance. They should be transparent, or at least painted white.

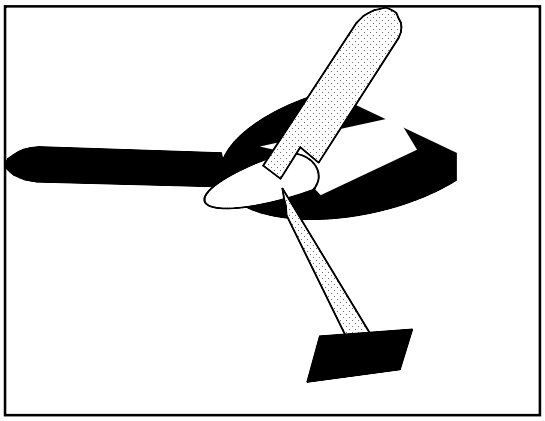

Figure 6. A black rectangle affixed to the tip of a single rotor blade.

Methods

The Pattern Electroretinogram (PERG)

Behavioral psychophysical methods to determine the optimal parameters of the patterns to minimize motion smear are extremely slow, time consuming, and labor intensive. A more rapid method, which has been used for psychophysical purposes, is the pattern electroretinogram (PERG) (Fitzke, et al., 1984,1985a, b; Hodos, et al., 1985; Porciatti, et al., 1991; Hodos et al., 2002; Gaffney and Hodos, 2003). The PERG is generated whenever there is a local contrast change on the retina, such as would be produced by a black bar moving across a white background. Likewise, it is generated as the retinal area goes from lighter to darker as the leading edge of the bar enters it and again as it goes from darker to lighter as the trailing edge exits it. Similar effects are achieved by the image of rotating blades as they pass through a given retinal area. Blank rotor blades generate a lower PERG amplitude than striped blades because they have a lower contrast against the background than do the stripes, which have nearly 100% contrast. In this case, the percentage of contrast is defined as $(L_L - L_D / L_L + L_D) \times 100$, in which L_L is the luminance of the brighter area and L_D is the luminance of the dimmer area. The pattern electroretinogram has been used to measure visual acuity, contrast sensitivity, and a variety of other psychophysical indicators (Fitzke, et al., 1984,1985a, b; Hodos, et al., 1985; Porciatti, et al., 1991; Hodos et al., 2002). In the studies that follow, the amplitude of the PERG was our measure of visibility of the blades. We examined this variable with a variety of anti-motion-smear and other patterns at various retinal-image velocities and against several types of stimulus backgrounds.

Apparatus

The apparatus used was the ENFANT visual electrophysiology system (Neuroscientific Corp., Farmington, NY). This instrument is capable of presenting a wide range of visual stimuli on a video display monitor and recording, amplifying, displaying, and analyzing electrical potentials such as those generated by the PERG. Among the analytical techniques available on this instrument are signal averaging (mean, root mean square, standard deviation, curve fitting, 95% confidence limits), variable high-pass and low-pass filtering, various regression analyses, Fourier analysis of frequency components, and others.

A variable-speed motor was fitted with 32-cm-long rotor blades made from 5-mm white foamboard. These were displayed against a background of the same material to provide a worst-case, minimal-contrast situation between blades and the background. Thus, the radius of the circle formed by the outer tips of the blades was 34 cm (including a 2-cm attachment device at the wheel hub). Since the viewing distance was 57.3 cm, at which distance an object 1 cm in length forms a retinal image that subtends a visual angle of 1° (see formula in Fig. 2), the visual angle subtended by the blades was 34º. Of equal relevance to this study, at this same distance an object rotating at 1 m/sec forms an image on the retina that has a velocity of 100 dva/sec, as will be seen by substituting in the formula in Fig. 2 the target velocity in m/sec for h and the distance in meters

(0.573) for d. A second set of blades of the same material was prepared with black stripes positioned according to the principle displayed in Fig. 3 or other striped patterns. The blades were viewed against a background of white posterboard with angular dimensions of 90º x 90º.

The sources of illumination were three tungsten halogen lamps positioned to minimize shadows. The average luminance of the white background was 752 cd/m^2. The brightest region was centered over the blades and had a luminance of 995 cd/m^2. The fall-off of luminance from the center to the extreme edges of the background was less than 0.25 log unit, which is relatively small in terms of brightness units based on data from pigeons (Hodos and Bonbright, 1972). The average luminance of the white bars was 614 cd/m^2 and that of the black bars was 37 cd/m^2. The contrast between the black bars and the white bars was 89% using the formula

$$\% \text{ contrast} = (L_W - L_B / L_W + L_B) \times 100,$$

in which L_W is the luminance of the white bar and L_B is the is the luminance of the black bar. All luminance measurements were taken with a Minolta luminance meter calibrated against a certified luminance standard traceable to the U.S. National Institute for Standards and Technology.

The diameter of the circle formed by the outer tips of the blades was 68 cm, which would form an image on the retina of 68°. This would be the same size retinal image that a 20-m diameter rotor would make at a distance of approximately 17 m. The birds, however, viewed only the lower third of the display, which had an angular subtense of about 56° wide by about 30° high, to approximate what a raptor might see approaching the faster-moving, outer region of a wind turbine rotor.

The rotation rate of the blades in RPM was measured by allowing the blades to interrupt a photocell light beam. The output of the photocell was led into the ENFANT apparatus, and the period of the resultant square waves was measured and converted to RPM.

Subjects

The subjects were 15 American kestrels (*Falco sparverius*) that were borrowed from the Patuxent Wildlife Research Center in Laurel, Maryland.

Procedure

In order to record the PERG, the subject was lightly anesthetized with 325-350 mg/kg IM of 20% chloral hydrate injected into the thigh or breast muscle, and 0.2 ml of vecuronium bromide was administered to the cornea over a 20-30 minute period to paralyze accommodation. The bird's head was then placed in a rigid metal head holder (stereotaxic instrument). In order to maintain general anesthesia at a light level, all pressure points and the interior of the ear canal had been previously treated with a long-lasting, local anesthetic cream (EMLA brand, 2.5% lidocaine and

2.5% prilocaine). The birds thus remained relaxed and comfortable throughout the duration of the experiment.

A 1.75-D lens was placed 2 cm from the eye to ensure that the retinal image of the blades would be in focus on the retina at the 57.3 cm viewing distance. The birds were unable to focus their eyes on the target because their accommodation mechanisms were paralyzed.

Platinum electrodes (0.5 mm diameter) were inserted in each upper eyelid so that the electrode made good contact with the sclera. Care was taken not to obscure the pupil. A third electrode was inserted in the skin of the scalp to serve as a ground. One eye was covered with a black patch. The electrode in this eye served as the reference electrode. This technique is minimally invasive, and the anesthesia depth is lighter than that required for major surgery.

The animal techniques used in this research were performed under approved protocols from the University of Maryland College Park Institutional Animal Care and Use Committee.

Location of the Fovea

To obtain the maximal amplitude of the PERG, it is necessary to have the rotating-blade display centered on the central fovea. By a series of experiments with various orientations of the head, we determined the azimuth and elevation of our experimental setup that would center the fovea on the blade display. With these coordinates for the location of the fovea, we have been able to center fovea on the stimulus display for any given kestrel.

Refractive State of the Eye

Before conducting any experiments in spatial vision, it is vital to carry out a preliminary study of the refractive state of the tested eye in each subject. If the eye has a refractive error (near-sighted or far-sighted) that remains uncorrected optically, the image on the retina will not be in focus and the results of the study will be compromised. The PERG was used for this procedure as well. Instead of the moving-blade display, however, the normal ENFANT monitor was used to present a series of square-wave gratings of various spatial frequencies. The bird's fovea was centered on this grating display. The method is based on the observation that PERG amplitude decreases as the spatial frequency of a grating stimulus increases. By increasing the spatial frequency (decreasing the width of the bars and spaces) until the PERG amplitude reached the noise level, the visual acuity of the subject can be obtained (Porciatti, et al., 1991). By determining which corrective lens gave the highest visual acuity (the precise equivalent of an optometrist's examination), not only did we measure the refractive state of the eye, we were assured that the image of the stimulus display was in focus on the retina. In general, we found American kestrels to be emmetropic; i.e., they required no optical correction for their vision, apart from the lens used to compensate for the short viewing distance and assure that the stimulus was in focus on the retina.

Results and Discussion

In this section, the results of each experiment will be reported and discussed. A general discussion of all the studies and their implications follows at the end of the report.

Visual Acuity of American Kestrels

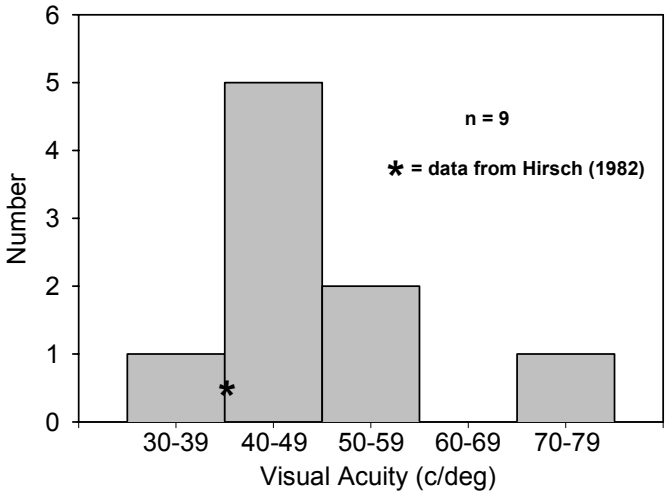

Figure 7. Visual acuity of nine American kestrels as determined by the PERG method. The data have been adjusted for the PERG's 37% underestimation of behavioral acuity (Hodos, et al., 2002). The asterisk indicates Hirsch's (1982) behavioral assessment of a single American kestrel.

A by-product of this preliminary study was an assessment of each subject's visual acuity at its best optical correction. Although acuity is not an issue for raptor-turbine collisions due to the increasingly larger images formed on the retina as the bird approaches a turbine, it is of interest given the effort expended on this topic by an industry-funded investigator, H. McIsaac. A detailed study of the acuity of our kestrels revealed that the median acuity was 29 cycles/degree. As a frame of reference, human 20/20 vision corresponds to 30 cycles/deg. PERG acuity, however, underestimates behavioral acuity by 37% (Hodos, et al., 2002; Peachy and Sieple, 1987). When corrected for this underestimation, the median corrected acuity was 47.3 cycles/degree (see Fig. 7). This value is closer to the behavioral estimate of Hirsch (1982) of 40 cycles/degree than is McIsaac's estimate of approximately 20 cycles/degree. These data are more fully described in Gaffney and Hodos, (2003).

Experiment 1. Threshold Visibility of a Simulated Turbine Blade Display

Eight blade velocities, ranging from 36-144 RPM, were used in the experiment. Table 1 shows the blade velocities in RPM, m/sec, and the velocity of the retinal image in dva/sec. Do these stimulus parameters realistically reflect the retinal-image velocities that would occur in the field? A 20-m-diameter rotor, for example, has a circumference of 62.8 m. At 70 RPM, the tip velocity is 264 km/hr (165 mph) or 73.3 m/sec. Its retinal-image velocity, however, depends on the distance at which it is viewed (see Figs. 2 and 3). At a distance of 32 m, the 20-m rotor will have a retinal-image velocity of 131 dva/sec, similar to our 36-RPM stimulus. At 8 m, it would have a retinal-image velocity of 525 dva/sec, similar to our 144-RPM stimulus (see Table 1).

Table 1. Blade Velocities and Retinal-Image Velocities Used in Experiment 1

A. Blade Velocity (RPM)	B. Blade-Tip Velocity (m/sec)	C. Blade-Tip Retinal-Image Velocity (dva/sec)
36	1.3	130
48	1.7	170
56	2.0	200
66	2.4	240
80	2.9	290
96	3.4	340
105	3.7	370
144	5.1	510

Blade Visibility

We have collected data from seven recording sessions (three measurements per session) from three American kestrels using the following stimuli: (1) blank blades; (2) blades with thin stripes in our staggered, anti-motion-smear pattern; (3) blades with thick stripes in anti-motion-smear, staggered pattern; (4) no stimulus (the eyes were covered so that they could not see the blades or anything else in order to obtain the physiological noise level, which was the baseline against which other measurements were compared). The thin stripes were 1.0 deg of visual angle in width and were spaced at 1.5-deg intervals. The thick stripes were 1.75 deg in width and were spaced at 2-deg intervals.

Fig. 8 shows the mean results of seven recording sessions with each of the four types of stimulus configuration. Three measurements typically were taken per session at each velocity. Each data point represents the mean of 19-21 PERG measurements in μV as a function of the velocity of the retinal image of the blade as it swept across the retina. Retinal-image velocity is in dva/sec. In the figure, the dotted line indicates the average PERG amplitude when the eyes are closed, which represents the level of equipment and biological noise and hence no visibility. Based on the results of studies of acuity and PERG amplitude, we are assuming that visibility varies linearly with a slope of 1.0 with the PERG amplitude that is above the noise level. Thus, doubling the amplitude above the noise level represents a doubling of visibility.

Our noise level was approximately 0.6 μV. If PERG amplitude above noise varies linearly with visibility, then for blank blades, the visibility at 130 dva/sec is about 1.0 (1.6 μV minus 0.6 μV). The visibility of the thick stripes was 2.2 (2.8 μV - 0.6 μV). The visibility of the thin stripes, however, was 4.2 (4.8 μV - 0.6 μV). Thus we can say that the thin, staggered stripes had a visibility that was approximately four times greater than the blank blades at 130 dva/sec. The thick stripes had a visibility that was nearly twice that of the blank blades. Stripe width thus appears to be an important variable because an increase in width from 1.0 to 1.75 deg resulted in a substantial decline in visibility.

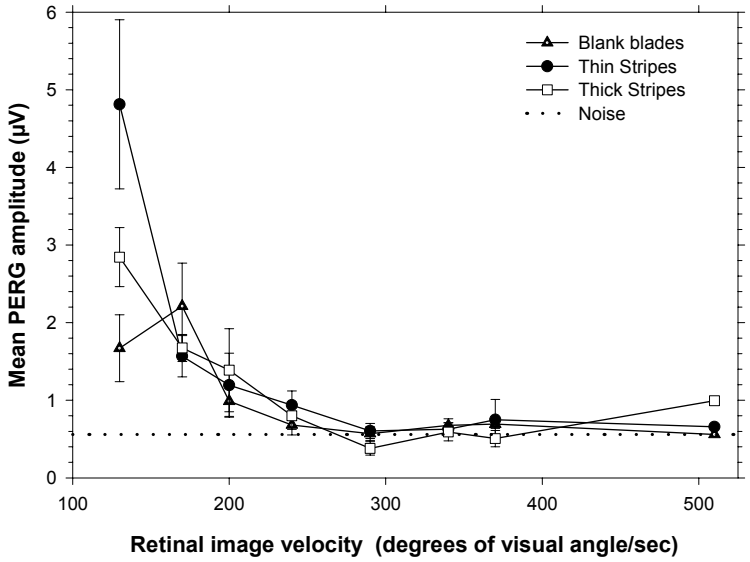

Figure 8. Mean PERG amplitude as a function of the velocity of the retinal image of the blade tip for three types of blade pattern and noise. Data points are the mean of seven sessions from three American kestrels. Three measurements typically were made per session. Each data point represents 19-21 measurements. Error bars are standard errors. The data points at 510 degrees/sec were collected from a single session (nine measurements per data point).

A Freidman-repeated measures, one-way analysis of variance was performed on the data at 130 dva/sec. The results were chi square = 13.2, d.f. = 3, $p < 0.004$. A Student-Newman-Keuls pairwise multiple comparison test indicated that the thin stripes were significantly more visible than the noise ($p < 0.05$) and the blank blades ($p < 0.05$). The thin stripes also were significantly more visible than the thick stripes ($p = 0.05$). Neither the thick stripes nor the blank blades were significantly different from the noise.

By 170 dva/sec, the visibility of the thin stripes dropped to 0.9 (1.5 μV - 0.6 μV), and by about 240 dva/sec, it dropped close to zero (i.e., to the noise level). At this velocity, the thick stripes had a visibility of 1.0 (1.6 μV minus 0.6 μV). In contrast, the blank blades had the greatest visibility of 1.6 at 170 dva/sec (2.2 μV minus 0.6 μV). However, none of these differences was significant from each other or from the noise. By 200 dva/sec and at all subsequent velocities, no differences between blades were significant, nor were any of the visibilities significantly different from noise. Hence, they were virtually invisible to the kestrel's eye.

What does this mean in practical terms? Fig. 9 gives some idea. In this figure, the X-axis has been changed to represent distance from the eye. We can make this conversion because for any moving stimulus, the retinal-image velocity increases linearly as the distance to the eye decreases. In this figure, we made this conversion for a hypothetical 20-m diameter turbine rotating at 45 RPM. The figure shows that at distances from the stimulus of 21 m, the three stimuli are clearly different, but the difference disappears when the difference shortens to 19 m and closer. By 15 m, the visibility of the blades has dropped effectively to zero, and the stimuli are virtually invisible to the kestrel. These distances only apply to a 20-m diameter turbine rotating at 45 RPM. Other combinations of diameters and RPMs would result in different values of the abscissa in Fig. 9.

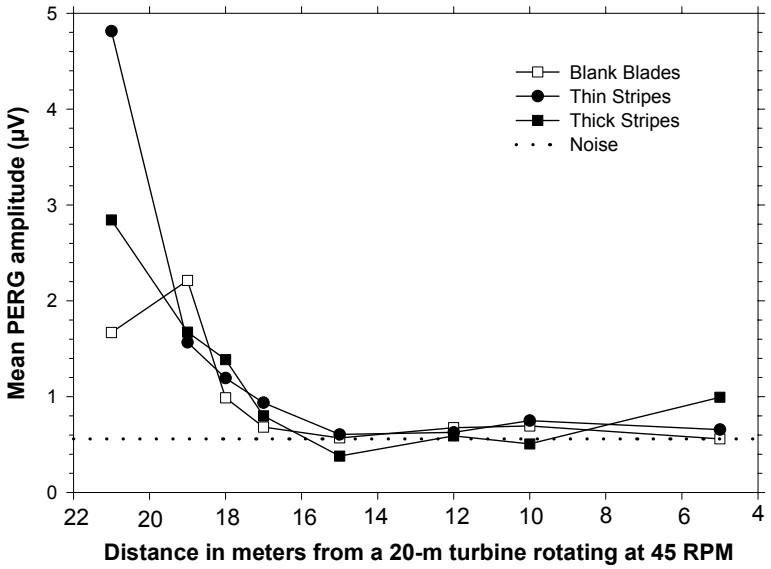

Figure 9. Blade visibility as a function of distance in the field from a hypothetical 20-m diameter turbine rotating at 45 RPM. Visibility data from Fig. 8.

How Useful Is Good Blade Visibility at 21 m?

A kestrel probably could safely maintain its position in front of a turbine at approximately 25 m (M. Morrison, personal communication). At a much closer distance, however, the bird would be at risk for not being able to avoid the blades should a sudden wind gust push it closer to them. Our data suggest that for the hypothetical case of a 20-m turbine rotating at 45 RPM, the thin-striped blades are visible at distances as close as 21 m. Moving closer to a distance of about 19 m, the thin-striped blades have lost their advantage over the blank blades. By about 15-17 m, all the blade types have been reduced to a transparent blur. Thus, once the temporal-processing ability of the retina approaches its limit, the fall-off in blade visibility is very rapid. For a larger, slower turbine, however, the minimum safe distance would increase. For example, a 60-m turbine with anti-motion-smear stripes rotating at 30 RPM would start to lose visibility at distances closer than 46 m. Blank blades would lose visibility at even greater distances. A more detailed description of the relationships among visibility distance, blade diameter, and RPM is given in the general discussion at the end of this report.

Whatever the visibility distance, as a bird moves closer to the turbine, the blades appear to be a transparent blur that the bird might interpret as being “safe”; i.e., as the bird gets closer, the threatening blades disappear and the bird might feel safe enough to approach or even attempt to

fly through the transparent visual smear. If anti-motion-smear patterns have any utility in averting avian collisions, their advantage would be that they keep the blades visible at closer distances than blank blades. Whether they would deter birds from flying into the zone of transparency that appears safe could only be determined by field testing.

Experiment 2. Achromatic Blade Pattern Types

The purpose of Experiment 2 was to evaluate a variety of blade patterns with anti-motion-smear properties. Six pattern types were used, as well as blank blades and a physiological noise condition in which the kestrel's eyes were covered with an opaque patch that prevented them from seeing any pattern. The stimulus presentation and recording methods were the same as for Experiment 1, except that the blades were presented at 130 dva/sec of retinal-image velocity, which is the retinal velocity at which the patterns are maximally visible. Three measurements were made of each pattern type during each recording session.

Figs. 10-16 demonstrate the blade patterns 2 through 8. (Pattern 1 consisted of no blade pattern; the bird's eyes were covered to determine the physiological noise level.) The left side of each photo shows the blades arranged radially as they would appear to the subjects of the experiment. The right side of the photo shows the blades side by side to reveal the presence or absence of anti-motion-smear properties. The thin stripes in Figs. 11, 13, and 15 were 1.0 deg in width. In Fig. 11, the spaces between the bars were 1.0 deg; in Fig. 13, the spaces were 1.25 deg; and in Fig. 15, the spaces were 1.7 deg. The thin stripes in Fig. 12 were 0.9 deg wide and were spaced 1.75 deg apart; the thick stripes in the figure were 1.75 deg wide and were spaced 3.5 deg apart. Fig. 14 shows progressive thick stripes that began at the blade base with a width of 3.75 deg, followed by widths of 3.25, 2.75, and 1.25 deg and continuing with uniform stripes of 0.9 deg width to the blade tip. Stripe spacings in this figure, beginning at the blade base, were 3.75, 2.40, 2.0, 1.75 deg, and then continued at 1.5-deg intervals to the blade tip.

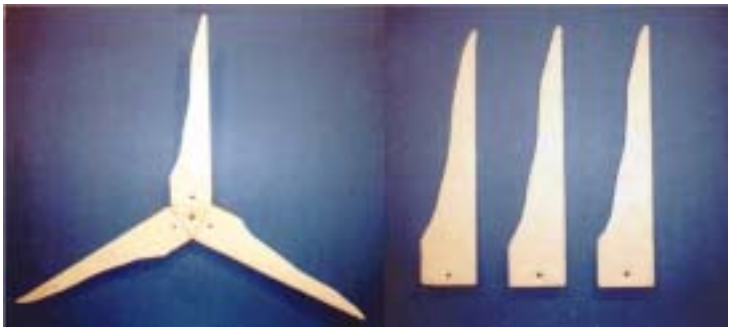

Figure 10. Blade pattern 2. Three blank blades.

Figure 11. Blade pattern 3. One blade, all thin stripes; two blank blades.

Figure 12. Blade pattern 4. Three blades staggered, thick and thin stripes. On the blade in the center in the photo on the right, the thick stripes begin halfway between the tip and the base of the blade. The location of the start of the thick stripes on the right and left blades have been staggered above and below the center of the center blade.

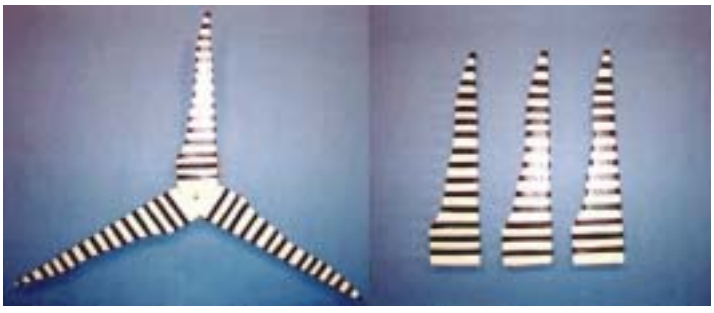

Figure 13. Blade pattern 5. Three blades, nonstaggered thin stripes.

Figure 14. Blade pattern 6. One blade; thick stripes at the inner half of the blade and thin stripes at the outer half; two blades blank.

Figure 15. Blade pattern 7. Three blades; staggered thin stripes.

Figure 16. Blade pattern 8. One blade, solid black; two blank blades.

The results are summarized in Fig. 17 and Table 2. Table 2 lists the eight stimulus conditions used in Experiment 2.

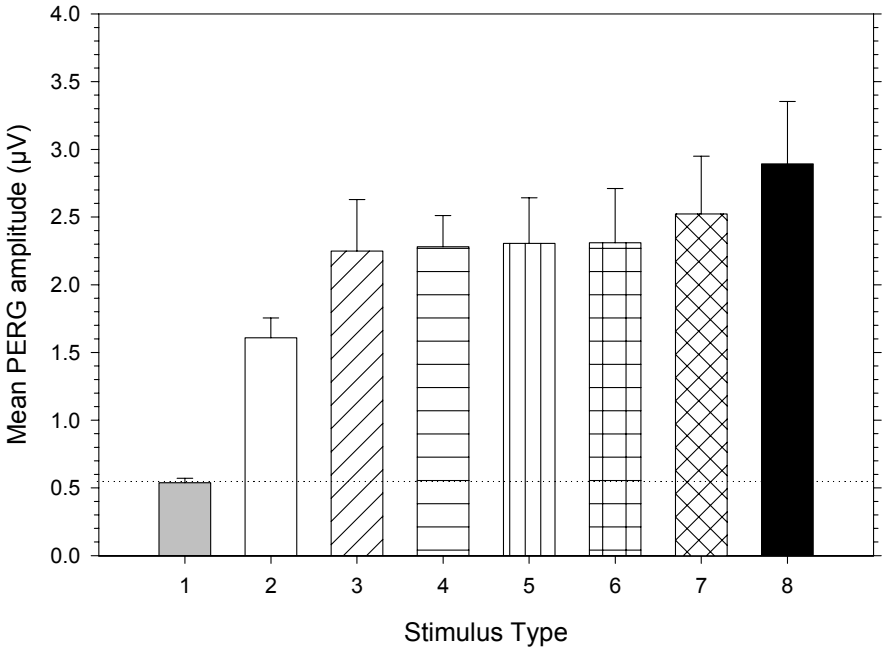

Figure 17. Mean PERG amplitude in response to eight stimulus patterns for six American kestrels recorded over five sessions. Three measurements were usually made per session. Total measurements per pattern type were 83-87. See Table 2 and text for a description of each stimulus type. Error bars are standard errors.

Table 2. Summary of PERG Amplitudes for the Seven Blade Patterns and Baseline Noise

Pattern No.	Pattern Type	Total PERG Amplitude (μV)	Visibility (μV above Noise)	Relative Visibility (μV above Blank)
1	noise (bird's eyes covered)	0.53	--	--
2	three blades, all blank	1.56	1.03	--
3	one blade, all thin stripes	2.24	1.71	0.68
4	three blades, staggered stripes, all thick and thin	2.28	1.75	0.72
5	three blades, non-staggered stripes, all thin	2.30	1.77	.074
6	one blade, stripes, all thick and thin; two blank blades	2.30	1.77	.074
7	three blades, staggered stripes, all thin	2.51	1.98	0.95
8	one blade, solid black; two blank blades	2.90	2.37	1.34

Pattern 1

Pattern 1 represents the mean of the noise-condition (eyes covered) recordings and constitutes the baseline against which other patterns are compared. In these experiments, the mean noise amplitude was 0.53 μV. We define visibility as the number of μV of PERG amplitude above the noise level and relative visibility as of μV of PERG amplitude above the amplitude of the blank blades.

Pattern 2

Pattern 2 is the array of three blank blades, which had a total PERG amplitude of 1.56 μV and a visibility (μV above the noise level) of 1.03. This is the standard against which other patterns must be compared and is the basis of our relative-visibility measure. We define relative visibility as the PERG amplitude (in μV) of a pattern above the PERG amplitude of blank blades.

Pattern 3

Pattern 3 had thin stripes of uniform thickness on one blade, and the other two blades were blank. Its total PERG amplitude was 2.24 μV, its visibility was 1.71, and its relative visibility was 0.68.

Pattern 4

Pattern 4 consisted of three blades with staggered stripes with thick stripes closer to the hub and thin stripes closer to the tip. This pattern had a PERG amplitude of 2.28 μV, a visibility of 1.75, and a relative visibility of 0.72.

Pattern 5

Pattern 5, which has a PERG amplitude of 2.30 μV, had a visibility of about 1.77 and a relative visibility of 0.74. It was composed of three blades with thin, unstaggered stripes of uniform thickness.

Pattern 6

Pattern 6 was a single-blade pattern with thick stripes near the hub and thin stripes near the tip combined with two blank blades. Its PERG amplitude was 2.30 μV, its visibility was 1.77, and its relative visibility was 0.74.

Pattern 7

Pattern 7 had staggered, thin stripes on all three blades and was the pattern used to collect the data shown in Experiment 1. The PERG amplitude of Pattern 7 was 2.51 μV, its visibility was 1.98, and its relative visibility was 0.95.

Pattern 8

Pattern 8 was a single, solid-black blade with two blank blades. This pattern had a PERG amplitude of 2.90 μV and a visibility of 2.37, compared to the visibility of 1.06 of the blank blades. Its relative visibility was 1.34, the highest of the six patterns.

A Friedman repeated measures analysis of variance was performed on the data. The result was chi-square = 128.7, d.f. = 7, $p < 0.001$. A Student-Newman-Keuls multiple comparison test, which compared each pattern to every other pattern, indicated that all the patterns were significantly more visible than the noise. In order to determine which of the patterns was significantly different than the blank blades (Pattern 2), a Dunnett Test for multiple comparisons with a control group (blank blades) was carried out. The Dunnett Test indicated that only Pattern 1 (the noise) and Pattern 8 differed significantly from the blank blades ($p < 0.05$).

In summary, by the indicators of total PERG amplitude and the visibility index, the single, black-blade pattern (Pattern 8) is approximately twice as visible as the three blank blades (Pattern 2). Note that the maximum PERG amplitudes in this experiment were not as high as those in Experiment 1. A number of factors may have contributed to this difference, such as intersubject variability, subtle differences in electrode position on the cornea, etc. In addition, a considerably greater number of measures were taken in Experiment 2 than in Experiment 1, which suggests that the Experiment 2 estimates of variability may be more accurate than those of Experiment 1.

Experiment 3. Visibility of Variously Colored Blades

To determine the effectiveness of color on blade visibility, we used chromatic stimuli specified by the R-G-B color system. The stimuli were uniform color fields printed using a Hewlett-Packard 2000, photo-quality, professional ink-jet printer. The red stimulus was 100% red at maximum saturation and intermediate brightness. The green stimulus was 100% green at maximum saturation and intermediate brightness. The blue stimulus was 100% blue at maximum saturation and intermediate brightness. The yellow stimulus was 50% red and 50% green at maximum saturation and intermediate brightness. The rotation rate of the blades was 130 dva/deg of retinal-image velocity, which is the retinal velocity at which achromatic patterns are maximally visible.

Fig. 18 summarizes our findings from data on seven kestrels. The blade configuration was similar to that shown in Fig. 16, except that one blade was colored or black. The data indicate that solid-color, single-blade chromatic stimuli are somewhat more visible than solid-black, single-blade stimuli. Yellow had the highest visibility. A Friedman repeated measures analysis of variance yielded a significant effect of color; chi-square = 99.1, d.f.= 6, p. = 0.028). A Dunnett test using the blank blades as a control revealed that the red, green, and black stimuli were significantly more visible than the blank blades ($p<0.05$). Even though yellow had the greatest visibility, it did not meet the criteria for being significantly different due to its greater variability.

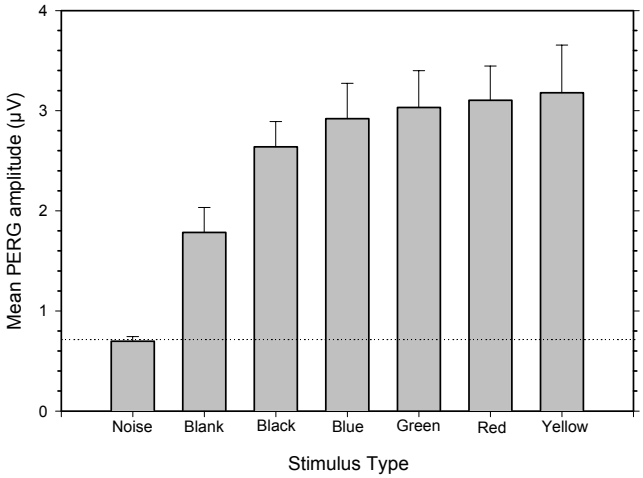

Figure 18. Mean PERG amplitude of six single-blade patterns with overall uniform colors for seven American kestrels using blades with uniform, overall solid colors. Three measurements were collected for three to five sessions for each bird. Each bar represents the mean of 66-69 measurements. Error bars are standard errors.

Experiment 4. Variability of Colored Blades Viewed against Colored, Naturalistic Backgrounds

Since our patterns had only been tested against a neutral white background, we were concerned about how visible our patterns might be against a multi-patterned, multi-colored background as would be encountered in the real world. We therefore tested the pattern series used in Experiment 3 against two "naturalistic" backgrounds. We used enlarged photographs of regions of wind-resource areas as a background against which the visibility of the various colored blades would be tested. The backgrounds were selected from the library of photos on the NREL Web site. We selected NREL PIX00906, a photo of California summer foliage depicting mainly yellow-browns and a deep-blue sky, and NREL PIX00052, a photo of California winter foliage depicting mainly greens, some browns, and a pale-blue sky. These are reproduced as Figs. 19 and 20. The photographs extended well beyond the perimeter of the blades.

Figure 19. NREL photo PIX00906 with a dark blue sky and wheat-colored foliage at ground level. Photo credit: David Parsons.

Figure 20. NREL photo PIX00052 with a pale blue sky and brown and green at ground level. Photo credit: Warren Gretz.

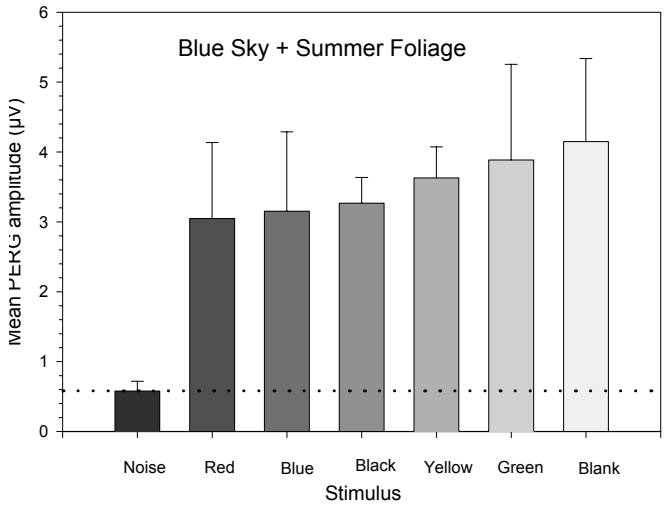

Figure 21. Colored-blade visibility against NREL photo PIX00906 as a background. Mean data from three kestrels recorded in five sessions for a total of 15 measurements per blade type. Error bars are standard errors.

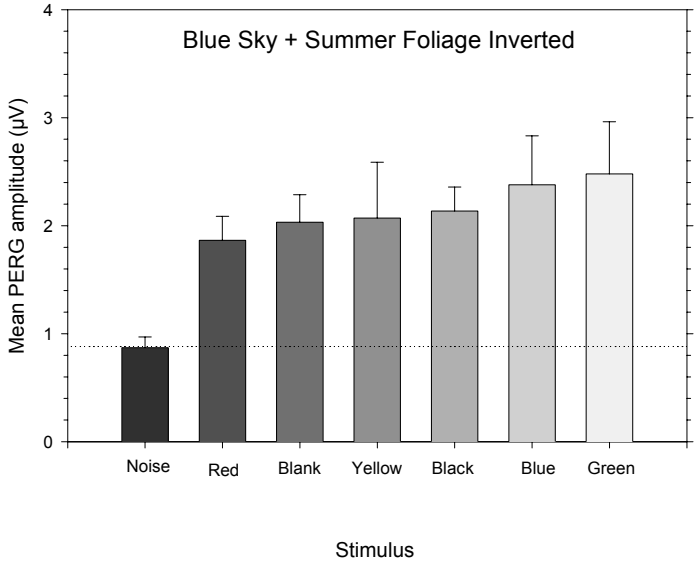

Figure 22. Colored-blade visibility with NREL photo PIX00906 inverted. The number of subjects and measurements are the same as for Fig. 21. Error bars are standard errors.

The results for the summer-scene background are shown in Fig. 21. The results indicate that against this scene, there are no significant differences among the stimuli. The blank stimulus shows an increase in variability over previous experiments and appears to be slightly more visible than the others. Determining whether this is a statistically reliable effect would require a large number of tests, given the variability in the data.

An inspection of the stimulus conditions revealed that the blades mainly were traversing the dark blue sky area and were not often passing over the yellow-brown ground. This is a view that a raptor would see when approaching the blades from below. We therefore repeated this test with the photo inverted so that the blades would mainly be seen against the yellow-brown foliage, as a raptor might see when approaching the turbine from above, and obtained the results shown in Fig. 22.

The result of inverting the background was that again there were no significant differences among these blade colors, although there appears to be a slight advantage of green and blue against the predominantly yellow-brown stimulus background.

Fig. 23 shows the visibility of the colored-blade patterns against the winter-foliage background (PIX00906) with pale-blue sky. Again, there are no significant differences among these blade colors, although green appears as the most visible.

Fig. 24 is a summary figure that combines the data of Figs. 21, 22, and 23. The results indicate that green, blue, and the blank stimulus have the highest visibility, but none of the colors is significantly different from black.

What can we conclude from these data? First, the data with complex colored and patterned backgrounds are variable. This suggests that the color and spatial patterning of the background will play a major role in the visibility of a particular stimulus. Second, the visibility of the blank blades increases considerably against this type of background. Third, the angle of approach of a raptor toward

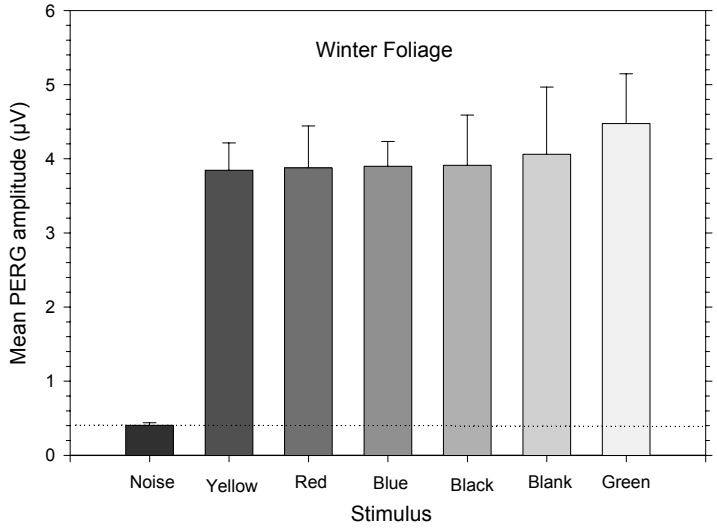

Figure 23. Colored-blade visibility with NREL photo PIX00052 as a background. Data are from three kestrels recorded over eight sessions. Each bar represents the mean of 24 measurements. Error bars are standard errors.

the blades will vary the background considerably and could have a major effect on blade visibility, depending on the color of the blade and the color/pattern combination of the background at the moment. The only color that seems to retain a relatively consistent level of visibility is black. The blank, for example, which has considerable visibility against intensely colored backgrounds, such as the deep-blue sky, would dramatically lose visibility against a background of clouds or hazy sky due to lack of contrast.

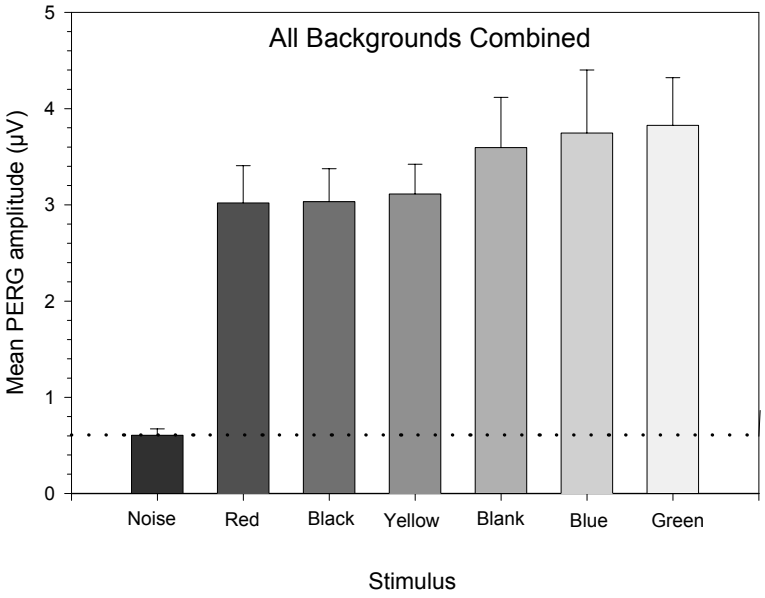

Figure 24. Data from Figs. 21, 22, and 23. Each bar represents three measurements from five kestrels over 18 sessions for a total of 54 measurements per blade color. Error bars are standard errors.

As a final test of colored blades and naturalistic backgrounds, we compared the visibility of solid green and solid black, single-blade patterns with black stripes (thick or thin) on a single blade or the blank blades. Also included was a single-blade pattern composed of thin silver reflective stripes, based on the notion that a simple reflector might provide enough variability in color contrast to be visible against the variegated naturalistic background. The stripes and spaces in this study were configured as in Fig. 11. The results, shown in Fig. 25, indicate that the thin, black stripes on a single blade are the most visible, but with the number of subjects tested (two) and the small number of recording sessions (four), the results are not significantly

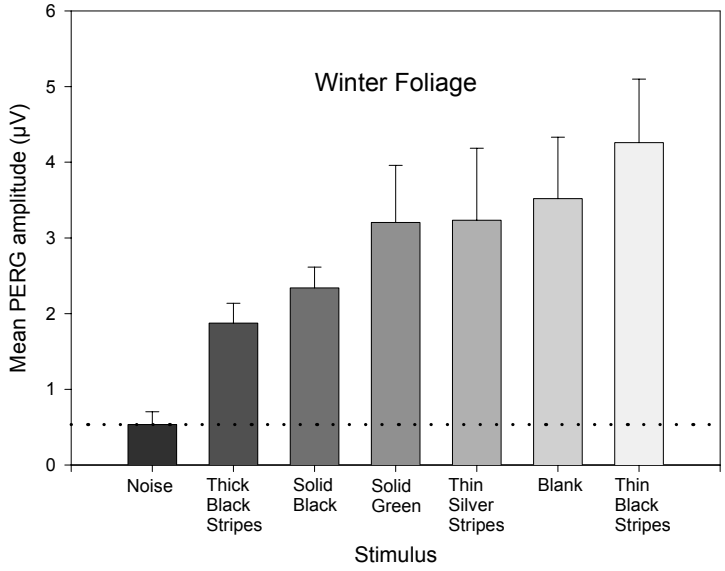

Figure 25. Comparison of the visibilities of several solid and striped single-blade patterns with NREL photo PIX00052 as a background. Data are the mean of two kestrels collected over four sessions for a total of 12 measurements per blade type. Error bars are standard errors.

different from a blank blade. A larger number of tests would be required in order for this difference to be statistically significant. Because the contract period was ending and additional experiments remained to be done, it was not possible to collect additional data.

In conclusion, our best estimate from all the data on colored blades against naturalistic backgrounds is that the single-blade, solid-black pattern or the three-blade, staggered, thin-stripe pattern is the stimulus that will have the maximum visibility under the widest variety of background coloration conditions. Although the blank blades generally do well against some natural colored backgrounds, such as a uniform, dark blue sky, they would have greatly reduced contrast against any light-colored background, and they would have extremely low contrast and thus low visibility against clouds or a hazy sky. Given these results and conclusion, the PI recommends that a field test be conducted using the single-blade, solid-black pattern. Although the thin-striped pattern performed better in this simulation, it is considerably more expensive to apply than a solid color because it would require precision application. The present evidence does not justify this additional expense.

Experiment 5. Visibility of Lateral Blade Stimuli against a Neutral White Background

A bird approaching a turbine at right angles to the long axis of the blade is presented with a very thin profile at very high velocity. It does not have the benefit of seeing the slower rotating, more central regions of the blades. A device attached to the blade tip at right angles to the long axis of the blade, such as the one shown in Fig. 6, would offer a larger profile to the bird. If it also had anti-motion-smear properties, it could increase the visibility of the tip region and help decrease the number of collisions. The purpose of this experiment was to evaluate the visibility of simulations of such devices. The devices that were attached to our blade simulations were black squares that subtended 6.5 x 6.5 deg of visual angle.

One Lateral Tip Device

The results, shown in Fig. 26, indicate no difference between laterally oriented blades with a single, black rectangle and those with no stimulus affixed to the tip. This finding was contrary to our expectations. Two possible explanations occurred to us to account for this finding: (1) a problem with depth of field, or (2) inadequate exposure time to each lateral tip device.

Depth of Field

Depth of field is the area in front and in back of the focal point of an optical system within which images are acceptably in focus. Thus, the blade tip might be in focus only for that short period when it was at closest to the eye. Because our optical system (kestrel's eye plus a supplementary lens to compensate for the short distance from the eye to the stimulus) is focused on the blade tip at its closest point along its circular path around the axis of the motor that drives the blades,

the blade tip is unlikely to be too close. It is possible, however, that when the blade is at its farthest from the eye (when it enters the test chamber at the top or leaves at the bottom), it may be at or beyond the limits of acceptable focus. If this is correct, it would mean that in the lateral view, the blade tips would be out of focus for some portion of each revolution. For studies of lateral approaches to blades, this could be a major limitation of the laboratory-simulation method, in which we use a short viewing distance to produce the retinal-image velocities that occur in the field with much larger, but slower rotating blades. In addition, our subjects were anesthetized and had paralyzed accommodation, which means that they could not change the focus of their eyes as the distance of the tip device increased and decreased on its arc. Because of the greater viewing distance and the freedom of the bird to accommodate, depth of focus is unlikely to play a role in viewing of lateral blade tips in the natural environment.

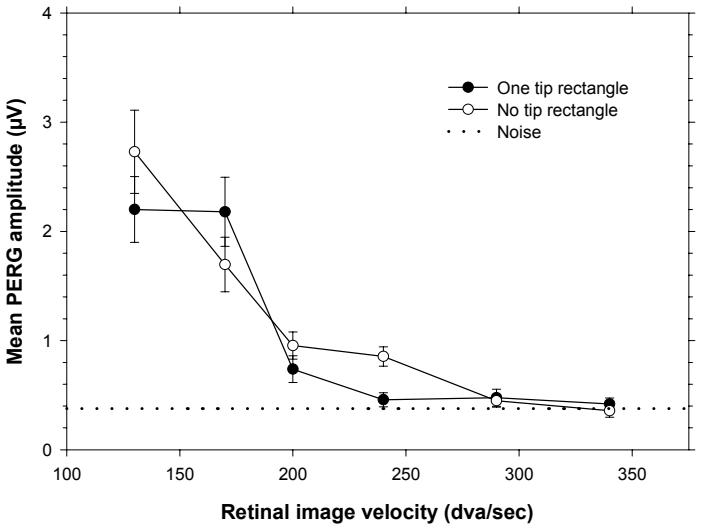

Figure 26. Visibility of a simulated turbine with a lateral tip attached to one blade. This stimulus is compared with a similar display with no tip device. Data are the mean of five sessions from four kestrels. Each data point represents 15 measurements. Error bars are standard errors.

Limited Exposure Time of the Tip in the Lateral View

Limited exposure time would seem to be a more likely explanation for the lack of difference between the stimulus conditions with and without lateral tip devices. When the blades are rotating at right angles to the axis of the eye, the retina is exposed to a wide range of retinal velocities: low near the hub of a blade array and high at the tip. This mixture of velocities almost certainly plays an important role in the total visibility of the blade array. In the lateral view, however, the retina is stimulated only by the high velocities at the tip of the blade. In order to test this possibility, we tested the kestrels with lateral tip devices attached to two or all three of the blades of the array. The additional rectangles should increase the total time that the retina is exposed to the rectangles, although there is the possibility that three rectangles would suffer from the very motion transparency that we are trying to avoid.

Two Lateral Tip Devices

Black rectangles were attached to two of the three blades; all other aspects of the experiment remained the same. As seen in Fig. 27, the data indicate that at low retinal-image velocities, the two-rectangle tip attachments resulted in increased visibility compared to the blank blades. A

Friedman one-way analysis of variance was performed on the data at 130 dva/sec. The results were chi square = 27.8, df=2, $p < 0.001$. A Student-Newman-Keuls pairwise multiple comparison test revealed that both the two tips and no tips displays were significantly different from noise ($p < 0.05$) and that the two-blade display was significantly different from the no-tips display ($p < 0.05$). The data thus indicate a clear advantage of the two-tip configuration at 130 dva/sec. At other retinal-image velocities, the data did not differ significantly.

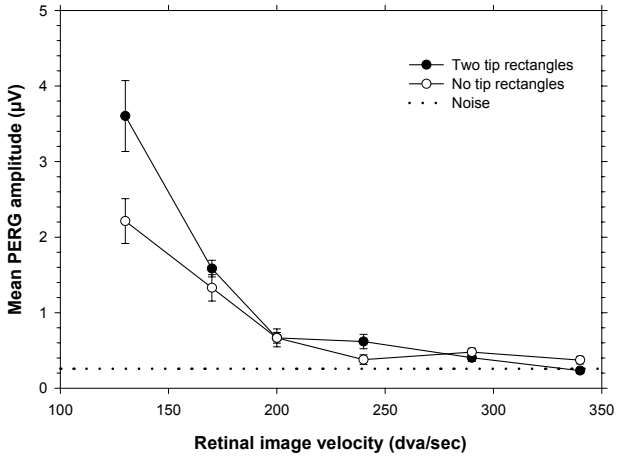

Figure 27. Visibility of a simulated blade display with two lateral tip devices compared to a similar display with no tip devices. Data are the mean of five sessions from five kestrels. Each data point represents 15 measurements. Error bars are standard errors.

Three Lateral Tip Devices

Fig. 28 shows that three lateral tip devices offer no greater benefit in visibility than does a single lateral tip device. The failure of three lateral devices suggests that this display lacks a sufficient duration of "off time" to function as an anti-motion-smear device.

Experiment 6. Visibility of Lateral Blade Stimuli against Colored, Naturalistic Backgrounds

The three-blade display with two lateral tip devices was the only configuration of lateral tip devices to show a difference in visibility at the 130 degrees of visual angle per second retinal image velocity from a similar display with no devices. To determine the effectiveness of the two-tip display against naturalistic backgrounds, we tested this configuration against a background

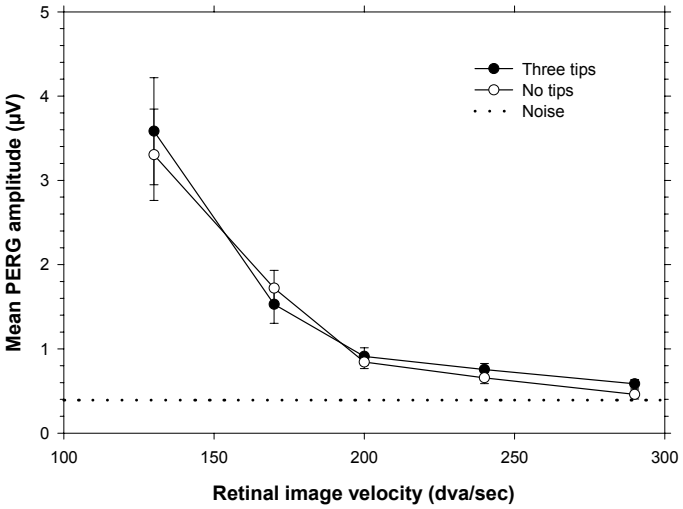

Figure 28. Visibility of a simulated blade display with a lateral tip device on each blade compared to a similar display with no lateral tip devices. Data are the mean of five sessions from five kestrels. Each data point represents 36 measurements. Error bars are standard errors.

of NREL photo PIX00052 (Fig. 20); i.e., California winter foliage (green), mottled brown earth tones, and a pale blue sky. Five kestrels were tested using the two-tip device with this stimulus as the background. The results of this experiment, shown in Fig. 29, indicate that against the naturalistic background, the difference between the two-tip device and the no-tip device has diminished somewhat. This finding suggests that against the naturalistic background, the two-tip device may be less effective. Fig. 30 shows the results of three lateral tips against a naturalistic background. The graphs indicate no difference between the two blade configurations.

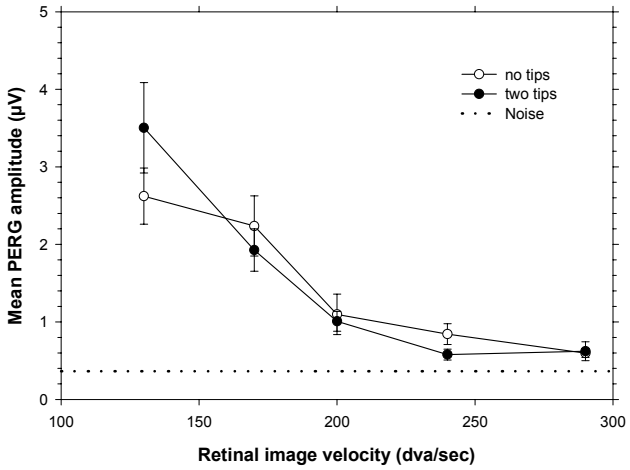

Figure 29. Visibility of a simulated blade display with two lateral tip devices viewed against NREL photo PIX00052 (Fig. 20) compared with a similar display with no lateral tip devices viewed against the same background. Data are the mean of two sessions from five kestrels. Each data point represents 30 measurements. Error bars are standard errors.

General Discussion

The Visibility of Rotating Blades

In this study, we evaluated the PERG visibility of seven blade velocities ranging from 36-144 RPM. These RPMs corresponded to tip velocities of 1.3-5.1 m/sec and tip-retinal-image velocities of 130- 510 (dva/sec). We found that for blank blades, the visibility at 130 dva/s is about 1.0 μV above the level of the physiological and instrument noise. By about 170 dva/s, the visibility had dropped by half, and by about 240 dva/sec, it has dropped close to zero (i.e., to the noise level). In contrast, we observed that thick stripes had a visibility of 2.2 μV above noise at 130 dva/s, whereas the thin stripes had a visibility of 4.2 μV above noise at the same retinal-image velocity. Thus we can say that the thin, staggered stripes had a visibility that is approximately four times greater than the blank blades at 130 dva/s. At 170 dva/s, all the patterns had about the same visibility. By 240 dva/s, all the patterns had dropped close to the noise level. Thereafter, all the stimuli essentially had no visibility as individual blades, but rather appeared blurry or transparent. We should note, however, that the thickness of the thin and thick stripes were arbitrary. We have no data to suggest what might be the optimum ratio of black stripe thickness to white stripe thickness. The significant results that we obtained were the result of scientific intuition (or perhaps just lucky guesses) about stripe width and spacing, rather than hard data. A parametric

study of stripe thickness and stripe spacing was beyond the scope of the proposed research, so we have no idea how much superior the results might have been had we determined the optimum stripe thickness and spacing between stripes. Such a study would have been lengthy, costly, and well beyond the budgetary constraints imposed by NREL. The data we have on stripe width (Figs. 8 and 17) suggest that we may have been close to the optimum width with stripe widths of 0.9 or 1.0 deg of visual angle. The spacing between stripes is another variable that would have benefited from a parametric analysis. For example, the lower visibility of the stripes in Experiment 2 compared to Experiment 1 and later studies may have resulted from the particular spacing of the stripes that were used. This discussion, of course, is entirely speculative.

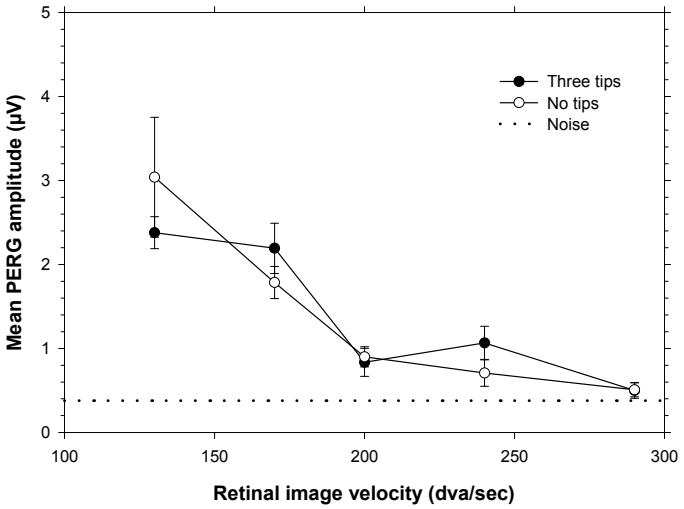

Figure 30. Visibility of a simulated blade display with a lateral tip device on each blade compared with a similar display with no tip devices. Both displays were viewed against the NREL photo PIX00052 (Fig. 20) as a background. Data are the mean of two sessions from five kestrels. Each data point represents 30 measurements.

Modeling Turbine Visibility Distance from Blade Diameter and Rotation Rate

In terms of the distance from the blades at which visibility would be maintained, using a hypothetical 20-m diameter turbine rotating at 45 RPM as an example, we modeled the distance at which visibility would be maintained (see Fig. 9). In our studies of blades against a neutral background, the results showed that the blank blades, thin-stripe blades, and thick-stripe blades would all be visible at a distance of 21 m, with the thin-striped blades being the most visible. By 19 m, the anti-motion-smear patterns would have lost their advantage over the blank blades. By 17 m, visibility for all three blade types would have dropped close to zero, and by 15 m, the blades would be virtually invisible to a kestrel.

The data in Fig. 8 and Fig. 9 indicate that a combination of the variables of blade diameter, rotation rate, and viewing distance that results in velocities of the retinal-image of the blade tip that exceed 130 dva/sec will result in motion smear and the apparent disappearance of the blade-tip image. Table 3, which is calculated from the relationships shown in Figs. 2 and 3, shows the distance in meters from turbine blades of various diameters (in meters) and rotation rates (in RPMs) that would result in the velocity of the retinal image of the blade tip being approximately 130 degrees of visual angle per second, which is the maximum retinal-image velocity at which anti-motion-smear stimuli are more visible than blank blades. The table indicates that a 20-m diameter turbine rotating at 45 RPM would have a retinal-image velocity of 130 dva/sec at a distance of 23 m, which should approximate a safe maneuvering distance while hovering in front of a turbine. On the other hand, for a 60-m turbine rotating at 35 RPM, the distance at which the

tip velocity was 130 dva/sec would be nearly 54 m. The tip would begin to lose visibility and the hazard to the bird would increase at a distance closer than 54 m.

Table 3. Distances from Turbines of Various Diameters and Rotation Rates to Produce a Tip Velocity of 130 Degrees of Visual Angle of the Retinal Image of the Blade Tip

	Turbine Diameter										
RPMs	10	15	20	25	30	35	40	45	50	55	60
5	1.28	1.91	2.56	3.19	3.83	4.47	5.11	5.75	6.39	7.03	7.67
10	2.55	3.83	5.11	6.39	7.67	8.94	10.22	11.50	12.78	14.06	15.33
15	3.83	5.74	7.67	9.58	11.50	13.42	15.33	17.25	19.17	21.08	23.00
20	5.10	7.66	10.22	12.78	15.33	17.89	20.44	23.00	25.56	28.11	30.67
25	6.38	9.57	12.78	15.97	19.17	22.36	25.56	28.75	31.94	35.14	38.33
30	7.65	11.49	15.33	19.17	23.00	26.83	30.67	34.50	38.33	42.17	46.00
35	8.93	13.40	17.89	22.36	26.83	31.31	35.78	40.25	44.72	49.19	53.67
40	10.20	15.31	20.44	25.56	30.67	35.78	40.89	46.00	51.11	56.22	61.33
45	11.48	17.23	23.00	28.75	34.50	40.25	46.00	51.75	57.50	63.25	69.00
50	12.75	19.14	25.56	31.94	38.33	44.72	51.11	57.50	63.89	70.28	76.67
55	14.03	21.06	28.11	35.14	42.17	49.19	56.22	63.25	70.28	77.31	84.33
60	15.30	22.97	30.67	38.33	46.00	53.67	61.33	69.00	76.67	84.33	92.00

Blade Patterns and Colors

Although several configurations of blade patterns were the most visible against the neutral white background, the single, solid-black blade would probably be the most visible against the widest variety of backgrounds. This pattern, which is consistent with the anti-motion-smear principle, offers the advantage of being the simplest to apply because it is an overall, uniform pattern that is applied to a single blade. Although various single-blade, solid colors, such as yellow, green, and red, appeared to offer slight visibility advantages over black when presented against an unpatterned white background, when viewed against backgrounds composed of photographs of naturalistic environments, (Figs. 19 and 20), green generally seemed to be the most visible. The differences between colors, however, were small and not statistically significant; therefore our conclusion is that black is probably the simplest and most cost-effective color to use. In one study, the display with a single-blade, thin-stripe pattern was the most visible against a naturalistic background (Fig. 25), but the number of observations was insufficient to achieve statistical significance.

Lateral Tip-Edge Devices

Although a single tip device (Fig. 6) was ineffective in enhancing visibility from a lateral viewpoint of the blades, the data showed that two-tip devices were superior to blades with no devices. As predicted by the theory of motion smear, three-tip devices were no more effective than no-tip devices. When shown against a naturalistic background, however, the two-tip device became less visible. In view of the ambiguous results with lateral tip devices against a naturalistic background, we cannot recommend them as practical collision-reduction devices without further research. One problem is that the size of the tip devices (6.5 x 6.5 deg of visual angle) was an arbitrary choice.

Given additional time and funding, we could have conducted a parametric study of tip device size to determine what the optimum size might have been. The visibility of an optimally sized device might have been better against a naturalistic background. In spite of the lack of statistical significance, the trend in the data of the two-tip device against a naturalistic background suggests that this might be a profitable area to pursue in future research, especially given the extreme hazard of a lateral approach to blade tips due to their motion smear and small profile.

How Natural Are the "Naturalistic Backgrounds"?

Although the naturalistic backgrounds represent images and colors similar to those that would be seen by a raptor flying over a wind resource area, they lack several important features that would be found in the natural visual world of a flying bird. The first is motion. The naturalistic backgrounds in the studies reported here were stationary, so important cues to distance, such as motion parallax (Goldstein, 1984), are absent. The visibility of the various stimuli used here might be completely different against the dynamic background seen by a flying bird compared to the static background of a still photograph. In addition, a closer approximation of nature might have been to use an aerial video of a wind resource area taken from the normal foraging altitude of an eagle, for example, and rear projected onto the background against which the blades were seen. Moreover, the results might have been different had we used stimuli in an optimal-visibility configuration against these naturalistic backgrounds.

Even motion enhancements of the simulation, however, would be without a second real-world feature: the true colors for birds. Birds have a tetrachromatric color system that uses four primaries compared to the trichromatic system of mammals (Jacobs, 1981). They see many more colors than we do, and they may see some colors differently than we do. In addition, many birds are sensitive to ultraviolet wavelengths (Cuthill, et al., 2000), which humans are incapable of seeing. Color photographs intended for the human eye, no matter how true to the natural scene the colors may appear to humans, would present a restricted range of colors to the avian eye. Many studies of avian perception have indicated that color is a critical variable for birds. Thus, these scenes may approximate the color appearance of the natural scene to a kestrel. Moreover, this restricted range of colors may have different effects on spatial vision and temporal summation in a bird than would occur when viewing the natural scene. Thus, although these background simulations give some suggestion of the complexity of the situation in comparison to a uniform, white background, they are a barely adequate substitute for field testing of the stimuli.

Usefulness of Visual Deterrents

An ideal visual deterrent for avian-turbine collisions is one that provides a highly visible warning signal to the bird and continues to provide high visibility as the bird nears the rotating blades. Our analysis of the problem from the velocity-detection literature and from our experiments reported here indicates that the physiology of the retina will not permit such a situation. Beyond a certain point, the velocity of the retinal images of the blades sweeping across the retina will overwhelm the retina's ability to keep up. The initial effect will be a smearing or blurring of the image of the blades, followed by their complete transparency, which could appear to be a safe place to fly, with deadly consequences for the bird. This would be especially true in the tip region of the blade, where velocity is the highest. Our analysis indicates that as the blade diameter increases, the minimum distance at which a visual deterrent will be visible increases. The lower rotation rates of the larger turbines mitigate that effect somewhat. But a 60-m diameter turbine would have to rotate at 15 RPM in order for its visual deterrent to be visible at 23 m, which is the visibility distance of a 20-m turbine rotating at 45 RPM (Table 3).

In the analyses reported here, we have considered that a kestrel might safely maneuver in front of a turbine at a distance of about 25 m (M. Morrison, personal communication). Although this distance is an educated guess not based on hard data, it can serve as a starting point for discussion. As we showed in Table 3, the minimum distance at which our thin-striped pattern is visible depends on the diameter and rotation rate of the turbine. Larger turbines tend to operate at lower RPMs, which keep the tip velocity more or less constant. Nevertheless, staggered-stripe patterns on the larger, slower turbines (which are the current trend in the wind power industry) will develop motion smear at greater distances than the smaller, faster models. Thus, paradoxically, the larger, slower turbines pose a greater hazard to birds in the region of the tip than do the smaller, faster turbines because they would become virtually invisible at distances well beyond the 25-m region.

Our data further suggest that among the achromatic patterns, the uniformly black, single-blade paired with two white blades would probably be the most effective anti-motion-smear pattern under the widest variety of conditions encountered in the field. The largest percentage difference between the visibility of a colored single-blade configuration and a solid black single blade is only about 9%. Much of this modest difference would probably be offset by the effects of color contrast. Green, for example, would be masked by green foliage in the background. Red, which would be quite visible against the blue of the sky, would be less visible in dim illumination, and its visibility could be easily reduced by earth tones in the background. White or black blades would have higher visibility against a dark blue sky, but a cloudy or hazy sky would eliminate this advantage.

Will These Patterns Deter Birds from Collisions?

When evaluating the usefulness of these patterns in deterring avian collision with wind turbines, remember that the research reported here has only told us something about what the kestrel sees or doesn't see. In other words, in these studies we have only investigated the ***physiological*** response of the eye to various patterns, not the ***psychological*** response of the animal to these stimuli; i.e., we have not investigated the brain's reaction to what the eye presents to it. It is the

animal's brain that interprets the retinal image and determines how the animal will react or not react to a given object in visual space. Thus, we have only investigated the visibility of these patterns and have no data regarding their deterrent properties.

The Need for Field Testing

The typical assumption is that if we do something to increase the visibility of the moving blades, then this will serve as a sufficient deterrent to a collision; but this assumption has not been tested in the studies reported here. Our studies have told us nothing about the kestrel's psychological reaction to what it sees. We have no data on whether these patterns, or any patterns, will deter birds from a collision course with moving blades. Our data reveal the likely cause of avian collisions with wind turbines, and they suggest techniques to increase the visibility of blades based on this understanding. Only a field test can tell us definitively whether a specific pattern will have the psychological property of being a warning stimulus. For example, without a field test, we have no idea whether some species of birds might find these patterns to be attractive rather than a deterrent, in which case they would be induced to approach them for closer investigation, with disastrous consequences for the bird. In our opinion, a field test is the essential next step to validate the deterrent properties of the proposed anti-motion-smear pattern.

Applications to the Wind Power Industry

A Useful Visual Deterrent to Avian Collisions?

The finding that anti-motion-smear patterns might increase the visibility of turbine blades at distances at which raptors could safely maneuver away from them should be of interest to the wind power industry. These data, however, only apply to laboratory conditions which mimic some aspects of optimum viewing in the field, such as bright illumination and good viewing conditions. We have no idea at present as to what extent these stimuli retain their improved visibility under sub-optimal viewing conditions, such as mist, rain, etc. Nor will they (or any other visual pattern, for that matter) retain their visibility once the animal gets close enough for the retinal-image velocity to approach 200 dva/sec, at which point the bird's retina has passed the limit of its ability to process temporally changing stimuli. Nevertheless, such patterns are worth testing in the field to determine whether the visibility advantages they offer will reduce avian mortality. A single, solid-black blade paired with two blank blades, or possibly a single, thin-striped blade paired with two blank blades, would probably be the most visible visual deterrent. We do not recommend the use of colored blades because of the additional expense and possible problems with background contrast.

Recommendations for a Field Test

To determine whether these laboratory studies have any utility in reducing avian collisions in the field, a field test must be conducted. The recommended pattern for this test would be the single,

solid-black blade and two blank blades. The duration of the test would be two years. If possible, black, lateral tip devices should be added to two of the three blades to protect against lateral approaches. Ideally, this should be a separate study, but it could be initially combined with a blade-painting study.

The solid black blade pattern is recommended for the field study because of the data in Fig. 24, which is a compilation of the studies with all the colored backgrounds. These data showed that the percentage difference between green (the most visible color against all the naturalistic backgrounds) and the solid-black single blade configuration was only 14.6%, which was not statistically significant. From an economic and practical point of view, black is the easiest and simplest solution because it requires no specific color matching.

If thin-striped blades were used, they could be applied in the single-blade configuration. The stripes should have the dimensions of those that were most effective in these studies; i.e., stripes that were 1.0 degree of visual angle in width and spaced 1.0 degree apart. The width and spacing in cm would be determined by the minimum distance at which the blades would remain visible based on the diameter of the circle formed by the turbine blade tips and the rotation rate given in Table 3. That distance would be entered into the equation for calculating visual angle, as shown in Fig. 2; i.e. visual angle = 57.3 h/d, in which h = stripe width or spacing and d = the minimum visibility distance. Thus, for a 60-m diameter turbine rotating at 30 RPM, Table 3 gives the minimum visibility distance 46 m. Setting visual angle in the equation to 1.0 degree, substituting 46 for d, and solving for h, we find that 1.0 deg = 57.3 x 0.8/46. Thus, at the minimum visible viewing distance of 46 m, a stripe of 80-cm width would subtend a visual angle of 1.0 degree.

For the field design, pairs of towers with the highest mortality rates should be selected. The towers do not need to be located in proximity to one another, but they should have approximately the same mortality rate. One member of the pair would get the single, solid-black blade pattern and the other would not. If any drop in mortality were seen in one member of the pair at the end of the first year's study period, then a cross-over design would be applied in which the black pattern would be moved to the other member of the pair to see if the drop in mortality followed the switch in the black blade location during the second year. If this effect occurred, this would be powerful and convincing evidence of the efficacy of the blade pattern as a deterrent.

References

Bex, P. J.; Edgar, G.K; Smith, A.T. (1995). "Sharpening of drifting, blurred gratings." *Vision Research,* 35, pp. 2539-2546.

Burr, D.C. (1980). "Motion smear." *Nature*, 284, pp. 164-165.

Burr, D.C.; Fiorentini, A.; Morrone, C. (1998). "Reaction time to motion onset of luminance and chromatic gratings is determined by perceived speed." *Vision Research*, 38, pp. 3681-3690.

Colson and Associates. (1995). *Avian interactions with wind facilities: A summary.* American Wind Energy Association.

Cuthill, I.; Partridge, J. C.; Bennett, A. T. D.; Church, S. C.; Hart, N. S.; Hunt, S. (2000). "Ultraviolet vision in birds." *Advances in the Study of Behavior*, 29, pp. 159-214.

Fitzke, F.W.; Hayes, B.P.; Hodos, W.; Holden, A.L. (1984). "Electroretinographic refraction of the pigeon eye." *Journal of Physiology* (London), 351, 21P.

Fitzke, F.W.; Holden, A.L.; Hayes, B.P.; Hodos, W. (1985). "Electrophysiological optometry using Scheiner's principle in the pigeon eye." Journal of Physiology (London), 369, pp. 17-31.

Fitzke, F.W.; Hayes, B.P.; Hodos, W.; Holden, A.L.; Low, J.C. (1985). "Refractive sectors in the visual field of the pigeon eye." Journal of Physiology (London), 369, pp. 33-44.

Gaffney, M.; Hodos, W. (2003). "The visual acuity and refractive state of the American kestrel (*Falco sparverius*)." *Vision Research,* 43, pp. 2053-2059.

Goldstein, B. (1984). *Sensation and Perception*. Belmont, CA: Wadsworth.

Hirsch, J. (1982). "Falcon visual sensitivity to grating contrast." *Nature,* 300, pp. 57-58.

Hodos, W. (1993). "The visual capabilities of birds." In Ziegler, H.P. and Bischof, H.J. (Eds.). Avian Vision, Brain and Behavior. Cambridge, MA: MIT Press, pp. 63-76.

Hodos, W.; Bonbright, J.C., Jr. "The detection of visual intensity differences in pigeons." *Journal of the Experimental Analysis of Behavior*, 1972, 18, pp. 471-479.

Hodos, W.; Fitzke, F.W.; Hayes, B.P.; Holden, A.L. (1985). "Experimental myopia in chicks: ocular refraction by electroretinography." *Investigative Ophthalmology & Visual Science,* 26, pp. 1423-1430.

Hodos, W.; Erichsen, J.T. (1990). "Lower-field myopia in birds is predicted by the bird's height: An adaptation to keep the ground in focus." *Vision Research*, 30, pp. 653-657.

Hodos, W.; Miller, R.F.; Fite, K.V. (1991). "Age-dependent changes in visual acuity and retinal morphology in pigeons." *Vision Research*, 31, pp. 669-677.

Hodos, W.; Ghim, M. M.; Potocki, A.; Fields, J. N.; Storm, T. (2002). "Contrast sensitivity in pigeons: a comparison of behavioral and pattern ERG methods." *Documenta Ophthalmologica*, 104, pp. 107-118.

Howell, J.A. (1991). *Visual experiment to reduce avian mortality related to wind turbine operations.* Final report to US Windpower, Inc., Livermore, CA.

Jacobs, G. H. (1981). *Comparative Color Vision*. New York: Academic Press.

National Renewable Energy Laboratory. (1994). *Proceedings of the National Avian-Wind Power Meeting*.

National Renewable Energy Laboratory. (1995). *Proceedings of the National Avian-Wind Power Meeting*.

Peachy, N.S.; Seiple, W.H. (1987). "Contrast sensitivity of the human pattern electroretinogram." *Investigative Ophthalmology and Visual Science*, 28, pp. 151-157.

Porciatti, V.; Hodos, W.; Signorini, G.; Bramanti, F. (1991). "Electroretinographic changes in aged pigeons." *Vision Research*, 31, pp. 661-668.

Steinman, R.M.; Levinson, J.Z. (1990). "The role of eye movement in the detection of contrast and spatial detail." In E. Kowler (ed) *Eye Movements and their Role in Visual and Cognitive Processes*. Amsterdam: Elsevier.

Thelander, C. G.; Rugge, L. (2000). "Examining relationships between bird risk behaviors and fatalities at the Altamont Wind Resource Area - a report on Phase II." *American Wind Energy Association, 2000 Conference Proceedings.*

REPORT DOCUMENTATION PAGE

Form Approved
OMB NO. 0704-0188

1. AGENCY USE ONLY (Leave blank)	2. REPORT DATE	3. REPORT TYPE AND DATES COVERED
	August 2003	Subcontractor Report: July 12, 1999 – August 31, 2002

4. TITLE AND SUBTITLE
Minimization of Motion Smear: Reducing Avian Collisions with Wind Turbines

5. FUNDING NUMBERS
WER3 3750
XAM-9-29211-01

6. AUTHOR(S)
W. Hodos

7. PERFORMING ORGANIZATION NAME(S) AND ADDRESS(ES)
University of Maryland
College Park, Maryland 20724-4411

8. PERFORMING ORGANIZATION REPORT NUMBER

9. SPONSORING/MONITORING AGENCY NAME(S) AND ADDRESS(ES)
National Renewable Energy Laboratory
1617 Cole Blvd.
Golden, CO 80401-3393

10. SPONSORING/MONITORING AGENCY REPORT NUMBER
NREL/SR-500-33249

11. SUPPLEMENTARY NOTES
NREL Technical Monitor: K. Sinclair

12a. DISTRIBUTION/AVAILABILITY STATEMENT
National Technical Information Service
U.S. Department of Commerce
5285 Port Royal Road
Springfield, VA 22161

12b. DISTRIBUTION CODE

13. ABSTRACT *(Maximum 200 words)*

Collisions with wind turbines can be a problem for many species of birds. Of particular concern are collisions by eagles and other protected species. This research study used the laboratory methods of physiological optics, animal psychophysics, and retinal electrophysiology to analyze the causes of collisions and to evaluate visual deterrents based on the results of this analysis. Bird collisions with the seemingly slow-moving turbines seem paradoxical given the superb vision that most birds, especially raptors, possess. However, our optical analysis indicated that as the eye approaches the rotating blades, the retinal image of the blade (which is the information that is transmitted to the animal's brain) increases in velocity until it is moving so fast that the retina cannot keep up with it. At this point, the retinal image becomes a transparent blur that the bird probably interprets as a safe area to fly through, with disastrous consequences. This phenomenon is called "motion smear" or "motion blur."

14. SUBJECT TERMS
wind energy; wind turbines; avian; avian collisions; motion smear

15. NUMBER OF PAGES

16. PRICE CODE

17. SECURITY CLASSIFICATION OF REPORT	18. SECURITY CLASSIFICATION OF THIS PAGE	19. SECURITY CLASSIFICATION OF ABSTRACT	20. LIMITATION OF ABSTRACT
Unclassified	Unclassified	Unclassified	UL